

- [7] M. Granström, M. Berggren, O. Inganäs, *Science* **1995**, 267, 1479.
- [8] C. S. Wang, M. Kilitziraki, L. O. Palsson, M. R. Bryce, A. P. Monkman, I. D. W. Samuel, *Adv. Funct. Mater.* **2001**, 11, 47.
- [9] A. C. Arias, M. Granström, K. Petritsch, R. H. Friend, *Synth. Met.* **1999**, 102, 953.
- [10] T. Granlund, T. Nyberg, L. S. Roman, M. Svensson, O. Inganäs, *Adv. Mater.* **2000**, 12, 269.
- [11] O. Inganäs, L. S. Roman, F. L. Zhang, D. M. Johansson, M. R. Andersson, J. C. Hummelen, *Synth. Met.* **2001**, 121, 1525.
- [12] G. Yu, J. Gao, J. C. Hummelen, F. Wudl, A. J. Heeger, *Science* **1995**, 270, 1789.
- [13] L. C. Chen, D. Godovsky, O. Inganäs, J. C. Hummelen, R. A. J. Janssens, M. Svensson, R. Andersson, *Adv. Mater.* **2000**, 12, 1367.
- [14] L. A. A. Pettersson, L. S. Roman, O. Inganäs, *J. Appl. Phys.* **1999**, 86, 487.
- [15] G. G. Malliaras, J. R. Salem, P. J. Brock, J. C. Scott, *J. Appl. Phys.* **1998**, 84, 1583.
- [16] G. Greczynski, T. H. Kugler, W. R. Salaneck, *Thin Solid Films* **1999**, 354, 129.
- [17] J. S. Kim, B. Läge, E. Moons, N. Johansson, I. D. Baikie, W. R. Salaneck, R. H. Friend, F. Cacialli, *Synth. Met.* **2000**, 111, 315.
- [18] L. S. Roman, O. Inganäs, T. Granlund, T. Nyberg, M. Svensson, M. R. Andersson, J. C. Hummelen, *Adv. Mater.* **2000**, 12, 189.
- [19] L. S. Roman, *Ph.D. Thesis*, Linköping University, Sweden **2000**.
- [20] M. Krogh, unpublished.

## Fabrication of High-Density, High Aspect Ratio, Large-Area Bismuth Telluride Nanowire Arrays by Electrodeposition into Porous Anodic Alumina Templates\*\*

By Melissa S. Sander, Amy L. Prieto, Ronald Gronsky,\*  
Timothy Sands, and Angelica M. Stacy

Wires with diameters of a few tens of nanometers or less are attracting considerable fundamental and technological interest because of their unique properties relative to the bulk. The properties of nanowires can be harnessed for a variety of applications, for example those requiring high current or redundancy, in dense arrays consisting of parallel wires. While several nanowire array fabrication methods have been developed, template-based approaches are well suited for producing arrays with uniform diameters and high aspect ratio wires.<sup>[1–4]</sup> In particular, porous anodic alumina templates have many desirable characteristics, including tunable pore dimensions over a wide range of diameters (~7–300 nm) and lengths (to >100 μm), good mechanical and thermal stability, and well-developed fabrication methods.<sup>[5–8]</sup> In this work, we have

employed anodic alumina templates to fabricate nanowire arrays of Bi<sub>2</sub>Te<sub>3</sub>, which have potential applications in thermoelectric devices due to the predicted enhanced thermoelectric properties of nanowires relative to the bulk.<sup>[9,10]</sup> We have deposited nanowire arrays by electrochemical deposition, which offers advantages over other deposition methods because it ensures electrically continuous wires and enables good control over stoichiometry. We describe a method to produce high-density (~5×10<sup>9</sup> cm<sup>-2</sup>), high aspect ratio (>1000), uniform, narrow diameter (45 nm ± 5 nm) Bi<sub>2</sub>Te<sub>3</sub> nanowire arrays over large areas (>1 mm<sup>2</sup>). This fabrication methodology may be applied to produce a wide range of both elemental and compound nanowire array systems.

There have been several previous reports of nanowire array fabrication by DC electrodeposition into porous anodic alumina templates,<sup>[11–16]</sup> however, there has been little emphasis on producing thick, dense, large-area templates suitable for facile assessment of the array properties over a homogeneous composite structure and potential incorporation into device structures. The fabrication of nanowire arrays with these characteristics is difficult due to the extremely narrow diameter, high aspect ratio pores, as well as the fragility of the templates. In previous reports, DC electrodeposition into alumina templates was used to produce nanowires by first fabricating a freestanding template and subsequently depositing an electrode layer for electrodeposition. In recent work, we used this technique to fabricate Bi<sub>2</sub>Te<sub>3</sub> nanowire arrays with a high degree of wire nucleation (in >80 % of the pores) and complete pore filling in ~10–20 % of the pores.<sup>[17]</sup> In the new fabrication approach reported here, several processing steps that lead to template damage or contamination have been eliminated, allowing reproducible fabrication of dense arrays with high aspect-ratio wires over large areas.

A schematic of the method employed to fabricate the nanowire arrays is shown in Figure 1. In this approach, first, one surface of an Al foil is mechanically polished, the thermal oxide layer is chemically removed, and a Ag film is sputter-deposited onto the Al to serve as an electrode in subsequent electrochemical deposition. Then, the Al is anodized to produce a nanoporous alumina template for nanowire array fabrication. The Al foil is prepared for anodization by mechanical polishing followed by electrochemical polishing in a method adapted from previous work.<sup>[18]</sup> After anodization, the template is transferred to an aqueous solution for Bi<sub>2</sub>Te<sub>3</sub> nanowire electrodeposition. Before electrodeposition, the template is allowed to soak for approximately one to two hours at room temperature in the 1 M HNO<sub>3</sub> solution in order to dissolve the barrier layer at the base of the pores (this step also causes slight pore widening). The oxide barrier layer in films prepared by anodization on the Ag substrate is thinner than in films prepared in aluminum, which allows for removal of the barrier layer without simultaneous dissolution of the entire anodic film.<sup>[19]</sup> We employ the deposition parameters for producing highly crystalline, textured, stoichiometric thin films of Bi<sub>2</sub>Te<sub>3</sub> established in prior work.<sup>[20–22]</sup> At the beginning of the deposition, the template becomes nearly uni-

[\*] Prof. R. Gronsky, Prof. T. Sands  
Department of Materials Science & Engineering  
University of California, Berkeley  
Berkeley, CA 94720 (USA)  
E-mail: rgronsky@socrates.berkeley.edu  
M. S. Sander,<sup>[+]</sup> A. L. Prieto, Prof. A. M. Stacy  
Department of Chemistry, University of California, Berkeley  
Berkeley, CA 94720 (USA)

[+] Current address: Institute of Materials Research and Engineering, 3 Research Link, 117602, Singapore.

[\*\*] This work was supported by the Office of Naval Research through a Multi-University Research Initiative under Contract No. N00014-97-1-0516. Electron microscopy was performed at the National Center for Electron Microscopy (NCEM), Lawrence Berkeley National Laboratory.

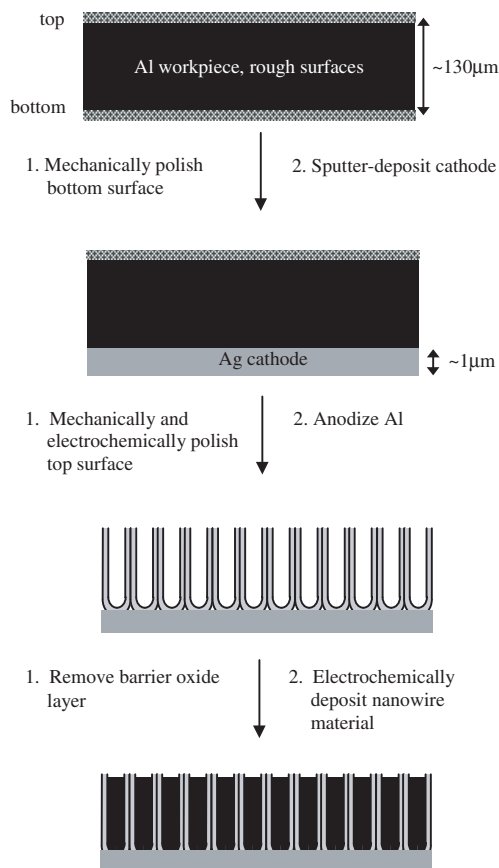


Fig. 1. Schematic of the process employed to produce nanowire arrays by DC electrodeposition into porous anodic alumina templates.

formly black, indicating that  $\text{Bi}_2\text{Te}_3$  has been deposited into the pores. After depositing for several hours, the entire surface of the template is gray, indicating that  $\text{Bi}_2\text{Te}_3$  has been deposited up to the top of the pores and overfilled the template.

Scanning electron microscopy (SEM) images of a  $\text{Bi}_2\text{Te}_3$  nanowire array/template composite in cross section are shown in Figure 2. The electrode layer is polished away to reveal the bottom surface of the composite (Fig. 2a). This image indicates that nucleation of wire material occurred in a significant percentage of the pores. However, after polishing away the overfilled  $\text{Bi}_2\text{Te}_3$  from the top of the pores, it is evident (Fig. 2b) that only a small number of pores filled completely to the top of the template. To determine the amount of nearly complete pore filling, the top surface of the template/array composite is mechanically polished down by  $\sim 5 \mu\text{m}$  (Figs. 2c and 2d). Approximately 70 % of the pores are filled to within  $5 \mu\text{m}$  of the top of the tem-

plate. The lack of complete pore filling may be due to variations in the rate of wire nucleation and/or wire growth, as well as blockage of wire growth due to defects in the pores of the alumina templates. The larger area image of the top surface of the array (Fig. 2d) is representative of images taken from various points across the top of  $\sim 1 \text{ mm}^2$  regions.

The structure along the length of the nanowires was determined from SEM images of templates cleaved along the wire axis. An image of wires within the alumina template is shown in Figure 3. The wires are dense, parallel, and of nearly uniform diameter along the length of the template. Defects resulting from the anodization process of the alumina are also visible, as indicated by the arrow in Figure 3.

The array/template composites were also assessed by energy-dispersive X-ray spectroscopy (EDS in the SEM) and X-ray diffraction (XRD). The composition of the arrays is approximately 2:3 Bi/Te as determined by EDS. XRD patterns from the arrays are dominated by the 110  $\text{Bi}_2\text{Te}_3$  peak, indicating that there is strong texturing along the wire axis. Two smaller  $\text{Bi}_2\text{Te}_3$  peaks (220 and 300) are also apparent, and a broad low-angle peak is attributable to the alumina template.

While these nanowire arrays have relatively high wire densities ( $\sim 5 \times 10^9 \text{ cm}^{-2}$ ), it may be possible to attain even greater pore filling to yield higher wire densities and maximize the nanowire contribution to the properties of the wire-matrix composite. One way to increase pore filling may be to improve the template quality using a two-step anodization process<sup>[23]</sup> or by nanopatterning the initial Al surface.<sup>[24]</sup> Such methods have been employed to produce very uniform diame-

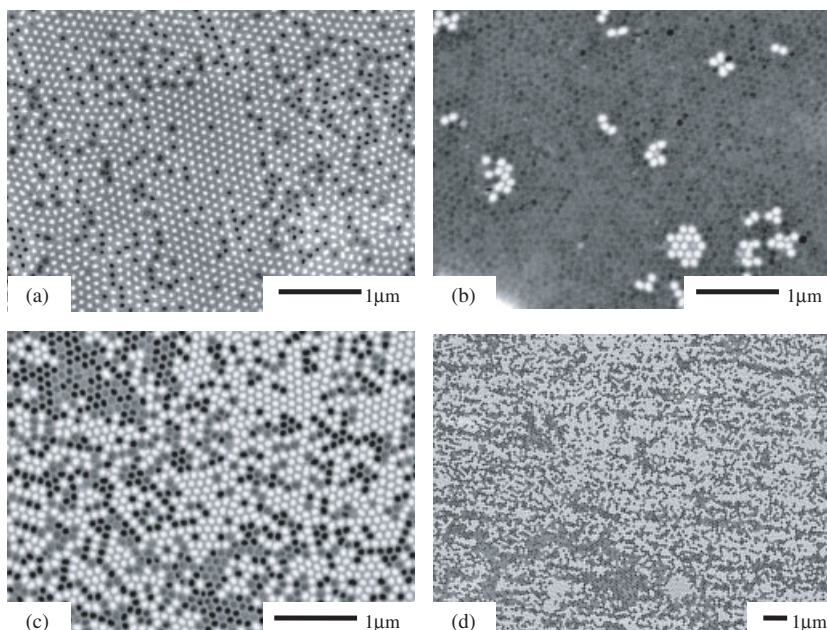


Fig. 2. SEM images of a  $\text{Bi}_2\text{Te}_3$  nanowire array composite in cross section. Light areas are due to  $\text{Bi}_2\text{Te}_3$  nanowires, dark regions are empty pores, and the surrounding gray matrix is alumina. a) Bottom surface of array after mechanically polishing away Ag electrode film. b) Top surface after polishing away overgrown  $\text{Bi}_2\text{Te}_3$ . c) Top surface after polishing off  $\sim 5 \mu\text{m}$  of the nanowire array composite. d) Larger area image of (c).

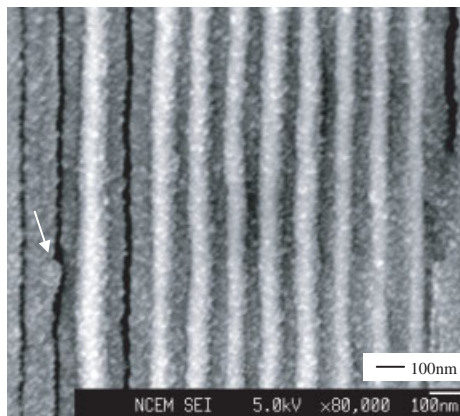


Fig. 3. SEM image of nanowire array composite along length of the wires. The arrow indicates a defect in the alumina template. (Slight surface texturing is due to a carbon film evaporated onto the specimen before imaging to prevent charging effects.)

ter, nearly perfectly cylindrical, well-ordered pores with a very low density of defects. It may also be possible to increase pore filling by improving mass transport in the deposition environment with ultrasonication during deposition and careful control over the bath temperature.<sup>[25]</sup>

In summary, by employing DC electrochemical deposition into porous anodic alumina templates, we have demonstrated a method to reproducibly fabricate high-density, high aspect ratio, narrow Bi<sub>2</sub>Te<sub>3</sub> nanowire arrays. SEM studies indicate that the individual wires are dense and parallel, with approximately 70 % of the pores of the anodic alumina templates completely filled, giving a wire density of  $\sim 5 \times 10^9 \text{ cm}^{-2}$ . The final composite thickness is  $\sim 55\text{--}70 \text{ }\mu\text{m}$ , and the average wire diameter is  $\sim 45 \text{ nm}$ , giving wire aspect ratios of greater than 1000. The composition of the arrays has been determined to be Bi<sub>2</sub>Te<sub>3</sub> by EDS and XRD. Because the array-template composites have a high wire density over a large area ( $>1 \text{ mm}^2$ ) and are relatively thick, they can be easily handled, and the properties of the nanowires can be readily assessed using standard bulk and thin film assessment techniques. Moreover these composites are suitable for direct incorporation into existing device structures for potential thermoelectric or other applications.

## Experimental

Nanochannel templates were produced from pieces of Al foil (99.9995 %, AlfaAesar). Coarse mechanical polishing (of the Al foil and the nanocomposite arrays) was performed with 1  $\mu\text{m}$  diamond polishing paste, and the composite arrays were finely polished prior to SEM imaging using a suspension of colloidal SiO<sub>2</sub>. Before anodization, the Al was electrochemically polished in a solution of 95 vol.-% H<sub>3</sub>PO<sub>4</sub>, 5 vol.-% H<sub>2</sub>SO<sub>4</sub>, 20 g L<sup>-1</sup> CrO<sub>3</sub> at  $\sim 85^\circ\text{C}$  with Pt gauze as the counter electrode at  $\sim 10\text{--}20 \text{ V}$  for  $\sim 10\text{--}30 \text{ s}$ . Immediately prior to electrode deposition and anodization, the Al working piece was immersed in a solution of 3.5 vol.-% H<sub>3</sub>PO<sub>4</sub>, 45 g L<sup>-1</sup> CrO<sub>3</sub> at  $\sim 90^\circ\text{C}$  for at least two minutes to remove any oxide from the surface. Typical anodization conditions were 30 V in 4 % oxalic acid at  $\sim 2\text{--}5^\circ\text{C}$ . After anodization, the template was rinsed with Millipore H<sub>2</sub>O and transferred without drying to the electrochemical deposition solution. Bismuth telluride was deposited at  $-0.46 \text{ V}$  vs. Hg/Hg<sub>2</sub>SO<sub>4</sub> (in saturated K<sub>2</sub>SO<sub>4</sub>) in an ice bath using concentrations of 0.075 M Bi and 0.1 M Te in 1 M HNO<sub>3</sub> in a three-electrode configuration consisting of the reference electrode, a Ag-sputtered alumina template as the working electrode assembly, and Pt gauze as the counter electrode. The reference electrode was

immersed in a separate beaker of 1 M KNO<sub>3</sub> and connected to the beaker containing the deposition solution by a KNO<sub>3</sub>/agar salt bridge.

The array structure was studied using a JEOL 6340F SEM, under typical working conditions of 5 kV. The arrays were coated with a thin carbon layer prior to imaging. EDS was conducted in a JEOL 35CF SEM. A Siemens D5000 diffractometer was employed for XRD.

Received: September 11, 2001  
Final version: February 20, 2002

- [1] C. R. Martin, *Science* **1994**, *266*, 1961.
- [2] C. R. Martin, *Chem. Mater.* **1996**, *8*, 1739.
- [3] A. Huczko, *Appl. Phys. A* **2000**, *70*, 365.
- [4] D. Routkevitch, A. A. Tager, J. Haruyama, D. Almalawi, M. Moskovits, J. M. Xu, *IEEE Trans. Electron Devices* **1996**, *43*, 1646.
- [5] H. Masuda, F. Hasegawa, S. Ono, *J. Electrochem. Soc.* **1997**, *144*, L127.
- [6] H. Masuda, K. Yada, A. Osaka, *Jpn. J. Appl. Phys.* **1998**, *37*, L1340.
- [7] A. P. Li, F. Müller, A. Birner, K. Nielsch, U. Gösele, *J. Appl. Phys.* **1998**, *84*, 6023.
- [8] O. Jessensky, F. Müller, U. Gösele, *Appl. Phys. Lett.* **1998**, *72*, 1173.
- [9] L. D. Hicks, M. S. Dresselhaus, *Phys. Rev. B* **1993**, *47*, 16631.
- [10] M. S. Dresselhaus, G. Dresselhaus, X. Sun, Z. Zhang, S. B. Cronin, T. Koga, *Phys. Solid State* **1999**, *41*, 679.
- [11] D. S. Xu, Y. J. Xu, D. P. Chen, G. L. Guo, L. L. Gui, Y. Q. Tang, *Chem. Phys. Lett.* **2000**, *325*, 340.
- [12] D. S. Xu, Y. J. Xu, D. P. Chen, G. L. Guo, L. L. Gui, Y. Q. Tang, *Adv. Mater.* **2000**, *12*, 520.
- [13] Y. Li, D. S. Xu, Q. M. Zhang, D. P. Chen, F. Z. Huang, Y. J. Xu, G. L. Guo, Z. N. Gu, *Chem. Mater.* **1999**, *11*, 3433.
- [14] X. Y. Zhang, L. D. Zhang, W. Chen, G. W. Meng, M. J. Zheng, L. X. Zhao, *Chem. Mater.* **2001**, *13*, 2511.
- [15] M. J. Zheng, L. D. Zhang, G. H. Li, X. Y. Zhang, X. F. Wang, *Appl. Phys. Lett.* **2001**, *79*, 839.
- [16] H. Masuda, M. Yotsuya, M. Ishida, *Jpn. J. Appl. Phys.* **1998**, *37*, L1090.
- [17] A. L. Prieto, M. S. Sander, M. S. Martin-Gonzalez, R. Gronsky, T. Sands, A. M. Stacy, *J. Am. Chem. Soc.* **2001**, *123*, 7160.
- [18] Z. B. Zhang, D. Gekhtman, M. S. Dresselhaus, J. Y. Ying, *Chem. Mater.* **1999**, *11*, 1659.
- [19] D. Crouse, Y. H. Lo, A. E. Miller, M. Crouse, *Appl. Phys. Lett.* **2000**, *76*, 49.
- [20] P. Magri, C. Boulanger, J. M. Lecuire, *J. Mater. Chem.* **1996**, *6*, 773.
- [21] P. Magri, C. Boulanger, J. M. Lecuire, "Electrodeposition of Bi<sub>2</sub>Te<sub>3</sub> Films", paper presented at the *Thirteenth Int. Conf. on Thermoelectrics*, Kansas City, MO, Aug. 30–Sept. 1, **1995**.
- [22] J. P. Fleurial, A. Borschchevsky, M. A. Ryan, W. Phillips, E. Kolawa, T. Kacisch, R. Ewell, "Thermoelectric Microcoolers for Thermal Management Applications", paper presented at *16th Int. Conf. on Thermoelectrics*, Dresden, Germany, Aug. 26–29, **1997**.
- [23] H. Masuda, K. Fukuda, *Science* **1995**, *268*, 1466.
- [24] H. Masuda, H. Yamada, M. Satoh, H. Asoh, M. Nakao, T. Tamamura, *Appl. Phys. Lett.* **1997**, *71*, 2770.
- [25] B. R. Martin, D. J. Dermody, B. D. Reiss, M. M. Fang, L. A. Lyon, M. J. Natan, T. E. Mallouk, *Adv. Mater.* **1999**, *11*, 1021.

## Molecular Recognition of Caffeine by Shell Molecular Imprinted Core–Shell Polymer Particles in Aqueous Media

By Stephen R. Carter and Stephen Rimmer\*

Molecular imprinted polymers (MIPs), first introduced by Mosbach<sup>[1,2]</sup> and Wulff,<sup>[3,4]</sup> are widely reported materials that can be used as biomimetic molecular recognition elements. They are prepared by polymerization of monomers bearing bonds to a template molecule. Removal of the template leaves

[\*] Prof. S. Rimmer, Dr. S. R. Carter  
The Department of Chemistry, University of Sheffield  
Sheffield, S3 7HF (UK)  
E-mail: S.Rimmer@Sheffield.ac.uk